

The Astrometric Imaging Telescope optical System

S. H. Pravdo,
S. Shaklan, and R. J. Terrile
Jet Propulsion Laboratory
California Institute of Technology
M/S 306-431
4800 Oak Grove Drive
Pasadena, CA 91109

C. Ftaclas and A. Nonnenmacher
Hughes-Danbury Optical Systems
hi/S 813
100 Wooster Heights
Danbury, CT 06810

G. D. Gatewood
Allegheny Observatory
U. of Pittsburgh
Observatory Station
Pittsburgh, PA 15214

E. I. Levy
Lunar and Planetary Laboratory
U. of Arizona
Tucson, AZ 85721

ABSTRACT

The Astrometric Imaging Telescope will detect extra-solar planetary systems with imaging and astrometry. The optical system contains a high-efficiency coronagraph and scatter-collimator lenses to detect Jupiter-size planets around nearby stars. The optical system also is distortion-free, tolerant to misalignments, and tolerant to optical surface contamination. This allows for the astrometric precision to detect Uranus-mass planets. A focal plane guider and fine guidance sensor are other elements of the optical design.

1. INTRODUCTION

The Astrometric Imaging Telescope (AIT) is a planned space-based observatory designed to detect and study planetary systems and circumstellar material around hundreds of nearby stars. The telescope provides light to two instruments that serially share the focal plane. The Optical Telescope Assembly (OTA) and elements of the Attitude Control System (ACS) and Science Instruments, comprise the optical system.

The OTA consists of a Ritchey-Chrétien telescope, baffles, structural elements, and an optical bench. The structure is a 3-tier, 18-bipod, graphite epoxy metering truss. It supports the primary and secondary mirrors and maintains their alignment. There are 4 rings including the titanium main ring that holds the primary. Figure 1 shows the OTA.

The telescope has a zero-distortion optical design and the mirror surfaces are figured to provide a high level of scatter compensation over the central 5 arcsec of the field of view. Table 1 shows the AIT optics design parameters.

The two Science Instruments use complementary techniques of imaging and astrometry to detect and study planetary systems. The first instrument, the Circumstellar Imager (CI), contains a high-efficiency coronagraph that reduces diffracted light from a central star by more than a factor of 1000. This, together with reduced scattering optics, allows direct imaging of Jupiter-size planets around nearby stars. The second instrument, the Astrometric Imager (AI), makes accurate measurements of the centroids of target stars and reference stars in

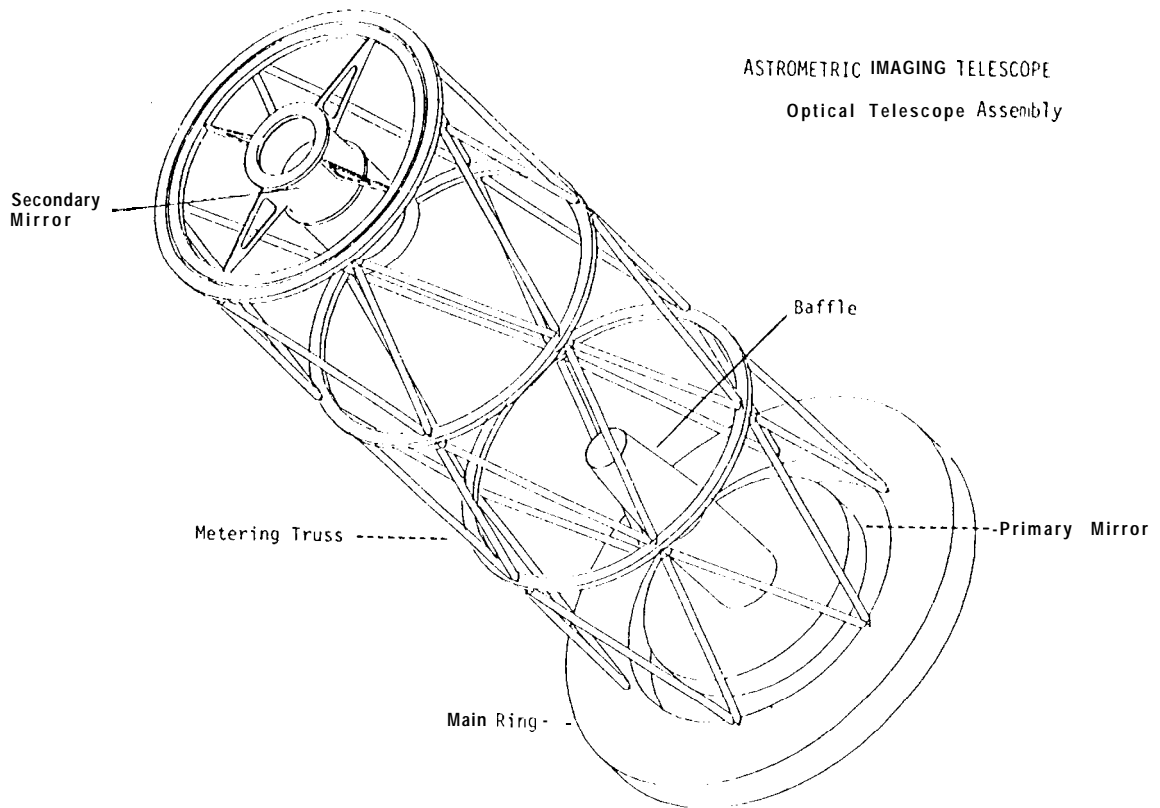


Figure 1: The AIT Optical Telescope Assembly

Table 1: AIT Design Parameters

Parameter	Value
Primary diameter	1.50 m
Primary focal length	7.48 m
Primary conic constant	-1.0787
Secondary Diameter	0.441"1
Secondary focal length	-2.96 m
Secondary conic constant	-4.9381
Primary-secondary separation	5.50 m
Back-focal distance	0.50 m
System focal length	22.64 m

Table 2: AIT Tolerancing

Perturbation	Tolerance
Secondary decenter	$\pm 250 \text{ }\mu\text{m}$
Secondary tilt	$\pm 30 \text{ arcsec}$
Secondary conic constant	>0.005
Primary conic constant	>0.01
Secondary-primary separation	>1 mm
Optical surface contamination	5% losses with 50 cm scale width showed negligible effects

fields. The zero-distortion optical design allows the system to be robust: accurate astrometric measurements are achieved even in the presence of reasonably expected optical aberrations and contamination of optical surfaces.

The attitude control system interacts with the rest of the optical system in two ways. First it receives light from the edge of the science field of view. Then it points the telescope and maintains the pointing stability to allow the science observations.

The following sections discuss in some detail each of the important and innovative elements of the AIT optical system.

2. TELESCOPE DESIGN

The astrometric principle behind the AI is that a target star can be accurately located relative to a fixed field of background stars. The advantages and disadvantages of this technique, along with several observational systems that utilize it, have been reviewed by Monet.¹ A time series of measurements of the target and reference star positions will then reveal whether the target star moves. For example, a star orbiting the center of mass of its planetary system will show a periodic motion relative to its reference field. Measurements of the stellar positions in the field, however, are complicated by field- and time-dependent effects of the optical system. For the AI, centroids of stellar images are used for positions. Distortion in the optics shifts the centroids leading to errors in the positions. Worse, the interaction of distortion with other aberrations such as astigmatism or with contamination of the optical surfaces can lead to time-varying positional errors. A zero-distortion optical system reduces this source of error and is therefore desirable.

Korsch described a Ritchey-Chrétien zero-distortion optical system.² His solution also had (to third order) zero spherical aberration and zero coma. The entrance pupil was placed at the primary mirror. This condition, along with the requirement for a positive back focal distance, drives the secondary-to-primary mirror diameter ratio to be at least 0.4. In fact a value near 0.55 was used in an early optical design. There are two consequences resulting from this large secondary design. First, the system is very tolerant to optical aberrations; i.e. positional errors remain small in the presence of macroscopic tilts, decenters, or surface contamination. This improves performance of the AI. But the second consequence has a negative impact on coronagraph performance: throughput of the coronagraph drops by a significant factor as the central obscuration increases, leading to an increase in the required observing times. For example the small secondary solution described below allows a factor of about 7 reduction in observing times.

To reduce the size of the secondary mirror, we searched for zero-distortion designs with the entrance pupil near the secondary. An additional constraint was introduced: the primary-to-secondary separation could be no larger than 5.5 m to fit into the required launch vehicle fairing. Manhart³ and Shu⁴ describe small-secondary solutions with Korsch and Korsch-like designs having the entrance pupil near the secondary. The design we chose is shown in Table 1 above. Small-secondary designs are less tolerant to aberrations than large-secondary designs, but nonetheless robust. Table 2 lists the tolerances of the AIT design.

The above tolerances apply when a 3-parameter fit to the reference fields is employed. Using a 6-parameter fit relaxes the tolerances further at the expense of increased observing time.⁵

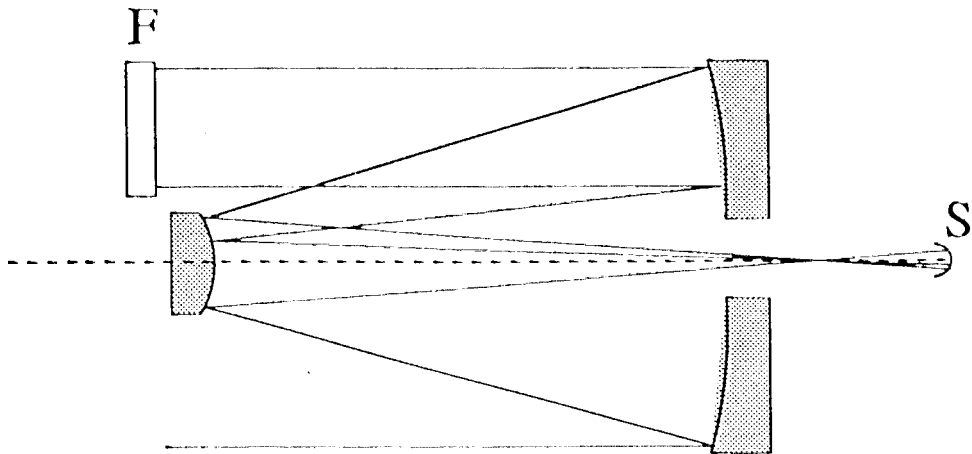


Figure 2: Test Configuration for Scatter-Compensated Optics. S: spherical mirror, F: reflecting flat

3. SCATTER-COMPENSATED SURFACES

The CL will produce direct images of Jupiter-size planets. The primary difficulty for the imaging is the contamination of planet light with background light from its central star. This is reduced in two ways. First, a hybrid coronagraph (see below) reduces the diffracted light at the planet position by a factor > 1000 . Second, scatter-compensated surfaces reduce scattered light at mid-spatial frequencies, also by a factor of 1000. Mid-spatial frequencies are critical because of the position of the planets relative to the stars on the focal plane. For example, a planet and a star 1-10 pc away with the Jupiter-Sun separation of 5 astronomical units (au.), will be separated by 5-0.5 arcsec, or about 50-5 diffraction radii. To achieve light scattering from stellar into planetary positions arises from optical figure errors with spatial frequencies 50-5 cycles per aperture. To achieve a factor of 1000 scatter reduction, the integrated surface figure error over these frequencies must be less than 3 \AA . The integrated power spectrum when extended over all spatial frequencies, assuming a cubic dependence, results in an integrated error of less than 7 \AA .

Deterministic polishing can create mirrors with the desired figure. The challenge is to measure the mirrors during and after the process to produce and verify the results. A study concluded that two methods could successfully measure the fabricated optics.⁶ In a “direct test” an annular zone on the mirror centered on the point of tangency of a reference beam is tested. The rest of the mirror is tested by measuring overlapping zones and stitching together the results. Melozzi et al. demonstrated this method.⁷ In a “shear test” the mirror is tested with a null corrector and then moved laterally and tested again. The slope of the wavefront is retrieved from the difference between measurements and integrated to yield the figure error. Either method when implemented would result in optics with the required scattering reduction over the entire field of view.

However, it was recognized by Ftaclas⁸ that for the specific problems of planet and circumstellar material detection, the full scattering reduction over the full field of view is overkill. The task is simplified when the field of view for the full scattering reduction is restricted to the central 5-10 arcsec where the circumstellar action is. First the primary and secondary mirrors are each figured to achieve a scattering reduction of about 100. Then the mirrors are tested together and one of them is figured to compensate for the errors of the other in the restricted field of view. Figure 2 shows the configuration for this test.

In the figure, S is the spherical front surface of an interferometer and F is a reflecting flat of about 60 cm. Fringes are formed between F and S, and by stitching overlapping regions a complete map of the aperture is formed. This test offers several advantages: only one optic needs the second level of figuring, the double-pass nature relaxes the knowledge requirement on the reference optics, and the optical system is tested as a unit. Calculations verify that this test addresses a sufficient field of view.

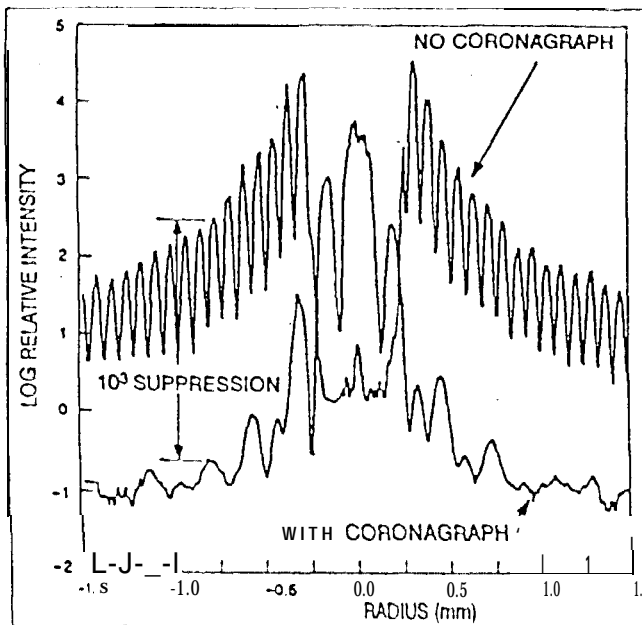


Figure 3: Laboratory Coronagraph Scattering Reduction Results

4. HYBRIDCORONAGRAPH

Diffraction reduction is a necessary step for imaging planets. The light from the diffraction wings of a star is still 10^5 times brighter than the light from a Jupiter-like planet at the planet location. The AIT requirement is to reduce the diffracted light by at least a factor of 1000 to allow signal detection at the 1% level. Standard coronagraphs consist of hard-edged occulting masks in the focal plane and Lyot⁹ stops in the pupil plane. These are limited in the amount of diffraction reduction in the central regions of the field. A hybrid coronagraph uses a graded occulting mask (e.g. with a Gaussian edge) to allow much larger diffraction reduction along with increased throughput near the center of the field of view. This is clearly superior for the circumstellar material and planetary detection problem.¹⁰ Even better performance may be possible with a graded Lyot stop.¹¹

Laboratory tests of a hybrid coronagraph demonstrate a factor of 1000 reduction in scattered light and verify the model. Figure 3 shows these results from the laboratory coronagraph.

The optical design of the AIT coronagraph is described by Shu.¹² It directs the light to a 76 mm diameter paraboloid which collimates the beam for the Lyot stops and filters. The back re-imaging optics are a Cassegrain telescope and two folding flats that direct the light to the CI CCD.

Modeling of the coronagraph shows that, in addition to reducing diffraction, it also reduces the scatter wings associated with low-order Zernike aberrations. This means that there are no extraordinary requirements with regard to focus, alignment, or pointing. This last issue leads into our discussion of the parts of ACS that relate to the optical system.

5. POINTING AND STABILITY

The ACS uses light provided by the main telescope optics to provide the pointing and stability required for the science observations. It contains a Focal Plane Guider (FPG) that functions like a star tracker and supports the AI observations. A second stage, the Fine Guidance System (FGS) supports the higher demands of the CI. Figure 5 illustrates the FPG/FGS configuration.

Light from the edge of the science field is picked off by a mirror and sent via relay optics to the FPG CCD.

ASTROMETRIC IMAGING TELESCOPE

Coronagraph

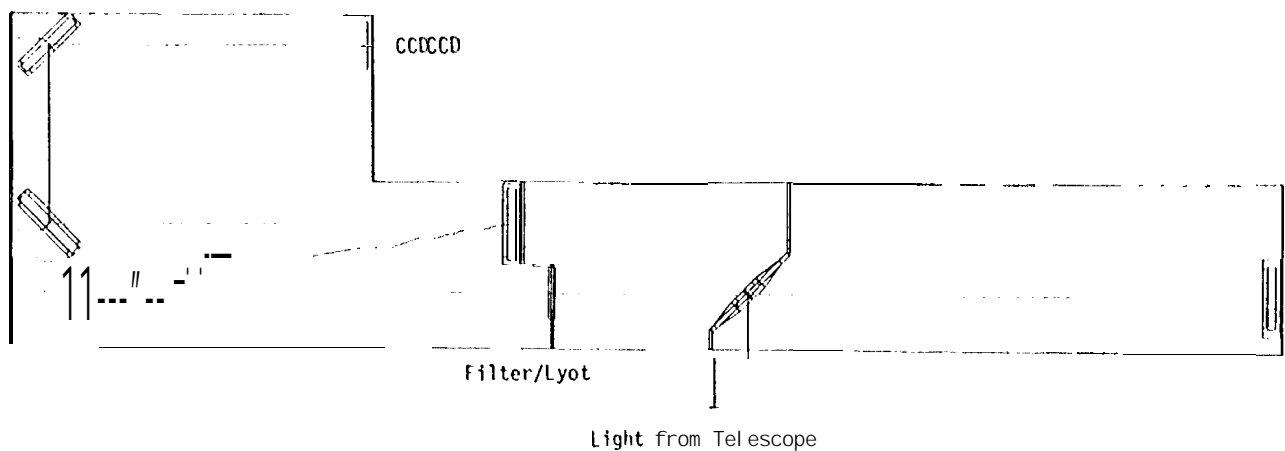


Figure 4: Coronagraph optical Layout

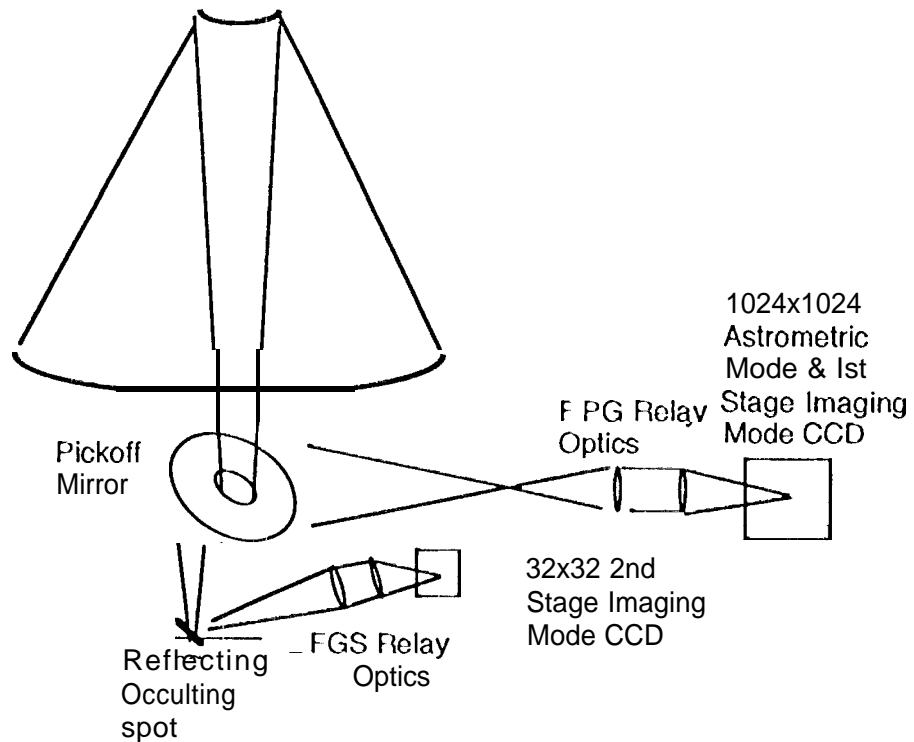


Figure 5: Focal Plane Guider and Fine Guidance System

This subsystem provides 0.2 arcsec pointing accuracy and stability (over 30 minutes). When the AI is observing this is the final stage of the pointing system. Since the AI makes relative measurements between stars in the same field, extraordinary pointing stability is not required. Care must be taken only that the stability in the frequency band in which the observations are taken (0.03-0.1 Hz) is maintained at the level of the required science accuracy.

When the CI is observing, an occulting spot, part of the hybrid coronagraph, is moved onto the optical axis at the focal plane. This spot reflects the rejected light from the central star into the FGS relay optics and then to the FGSCCD. The FGS subsystem provides 0.05 arcsec pointing accuracy and 0.01 arcsec stability (over 30 minutes) and is the second stage of the pointing system. This stability is sufficient to keep the central star on the occulting spot without significant leakage around the edges. As mentioned above the model indicates that low order Zernike aberrations in this system are suppressed by the coronagraph.

This level of pointing stability is similar to that obtained with the Hubble Space Telescope.^{13,14} The problem of pointing is considerably eased for AIT for several reasons. First AIT is a smaller telescope (about 2500 kg compared to HST 11000 kg) with lower moments of inertia. Next, there have been considerable advances using CCDs in pointing systems over the last several years (e.g. ref. 15). Finally, the "guide" star is automatically available in Al'l'/CI observations, it is located in the center of the field, and it is bright, at least 8th mag.

6. ACKNOWLEDGEMENTS

This work was carried out at the Jet Propulsion Laboratory, California Institute of Technology, under contract with the National Aeronautics and Space Administration. Ken Lau assisted in the preparation of this manuscript.

References

1. Monet, D. G., 1988, *Ann. Rev. Astron. Astrophys.*, **26**, 413.
2. Korsch, D. 1989 in *Astrometric Telescope Facility (ATF) FY'89 Final Report*, J }'1, 1>-7113 (ed. by S. Pravdo), p. 17. (Internal Report).
3. Manhart, I. 1993 in *Astrometric Imaging Telescope 1992 Final Report*, JPL D-10760 (ed. by S. Pravdo), p. 253. (Internal Report).
4. Shu, K.-L. 1993 in *Astrometric imaging Telescope 1992 Final Report*, JPL D-10760 (ed. by S. Pravdo), p. 253, (Internal Report).
5. Shaklan, S. and Pravdo, S. II. 1993, *Proc. of S. P. I. E.: Space Astronomical Telescopes and Instruments 11*, **1945**, 505.
6. Ftaclas, C. et al. 1992 *Astrometric Imaging Telescope Project Report: Final Report for the AIT Metrology Definition Study*, FIR B1 1-0348, Hughes Danbury Optical System to .11'1.
7. Melozzi, M. et al. 1993, *Optical Engineering*, **32**, 1073.
8. Ftaclas, C. 1993 in *Astrometric imaging Telescope 1992 Final Report*, J }'1, 1L10760 (ed. by S. Pravdo), p. 279. (Internal Report).
9. Lyot, B. 1933, *M. N. R. A. S.*, **99**, 580.
10. Ftaclas, C. et al. 1994, *Ap. and Sp. Sci.*, in press.
11. Nonnenmacher, A. 1993 in *Astrometric Imaging Telescope 1992 Final Report*, J 1'1, D-10760 ed. by S. Pravdo), p. 333. (Internal Report).
12. Shu, K.-L. 1993 in *Astrometric Imaging Telescope 1992 Final Report*, J 1'1, D-10760 (ed. by S. Pravdo), p. 343. (Internal Report).
13. Bradley, A. et al. 1991, *P. A. S. P.*, **103**, 317.
14. Burrows, C. J. et al. 1991, *Ap.J.(Letters)*, **369**, 1,21.
15. Stanton, R. II. et al. 1993, *Proc. of S. P. I. E.: Space Guidance, Control, and Tracking*, **1949**.